

## On the circulation in the Puerto Morelos fringing reef lagoon

C. Coronado · J. Candela · R. Iglesias-Prieto ·  
J. Sheinbaum · M. López · F. J. Ocampo-Torres

Received: 18 July 2006 / Accepted: 25 October 2006 / Published online: 7 February 2007  
© Springer-Verlag 2007

**Abstract** For a period of 22 months beginning in September 2003, an array of four current profilers were deployed on the Puerto Morelos fringing reef lagoon, a microtidal Caribbean environment characterised by the influence of the Yucatan Current (YC) and a Trade Wind regime. The dataset includes water currents, bottom pressure, and surface waves complemented with coastal meteorological data and surface currents from an acoustic Doppler current profiler moored 12 km offshore. Normal circulation conditions consisted of a surface wave-induced flow entering the lagoon over a shallow reef flat and strong flows exiting through northern and southern channels. This wave induced flow was modulated by a low-frequency sea level change related to a geostrophic response to the YC variability offshore, with tidal and direct wind forcing playing additional minor roles. Under extended summer low-wave height conditions, together with a decrease in sea level from the intensification of the

offshore current, the exchange of the lagoon with the adjacent ocean was drastically reduced. Under normal wave conditions ( $H_S = 0.8 \pm 0.4$  m, mean  $\pm$  SD), water residence time was on average 3 h, whereas during Hurricane Ivan's extreme swell ( $H_S = 6$  m) it decreased to 0.35 h.

**Keywords** Fringing reef lagoon · Hydrodynamics · Surface waves · Residence time · Along shore current modulation

### Introduction

The Mexican Caribbean Sea includes an important portion of the Mesoamerican Reef, at the core of the most important tourist centre in Mexico. Puerto Morelos is situated in the northern part of this extensive barrier-fringing reef that extends from Honduras to the Yucatan Channel; it is a small fishing village and harbour that has been threatened in recent years by development and pollution. Urbanisation for tourism infrastructure and residential housing is rapidly increasing, resulting in landfill and deforestation of the wetlands. Both are expected to increase further, as the government considers additional tourist resorts on the coast and an industrial zone landward (Ruíz-Rentería et al. 1998). At present, Puerto Morelos remains relatively pristine, but growing in the shadow of Cancún, it is struggling to avoid the rampant development and the ensuing environmental degradation that taints its northern neighbour.

Circulation in reef systems is typically driven by a combination of tidal and wind-driven flows, and water currents induced by the breaking of wind-waves over

---

Communicated by Environment Editor R. van Woesik.

---

C. Coronado (✉) · J. Candela · J. Sheinbaum ·  
M. López · F. J. Ocampo-Torres  
Departamento de Oceanografía Física,  
División de Oceanología, Centro de Investigación  
Científica y de Educación Superior de Ensenada,  
Km 107 Carretera Tijuana-Ensenada, Ensenada,  
Baja California 22860, México  
e-mail: coronado@cicese.mx

R. Iglesias-Prieto  
Unidad Académica Puerto Morelos,  
Instituto de Ciencias del Mar y Limnología,  
Universidad Nacional Autónoma de México,  
Apdo. Postal 1152, Cancún,  
Quintana Roo 77500, México

the reef flat (Symonds et al. 1995; Hearn 1999). For Caribbean fringing reefs, wave overtopping on the reef crest and the resulting flow is considered to be the main driving mechanism of the circulation (Roberts et al. 1992), whereas the tide is thought to be the main driving force in fringing reefs in the Great Barrier Reef because of large tidal ranges (Yamano et al. 1998; Wolanski 2001). The importance of wind on the circulation in coral reefs has been investigated on deep atoll lagoons (Atkinson et al. 1981; Tartinville et al. 1997), but its effect on the circulation of shallow fringing reefs has been discussed somewhat less because currents driven by local winds in lagoons are often weaker than the strong tidal and wave driven currents. Also, most studies of water circulation in coral reefs have been made in Trade Wind areas where wind and swell are often constant. Nevertheless, Yamano et al. (1998) showed that the effect of wind may be important in shallow lagoons subjected to wind events characterised by a sudden change in magnitude and direction.

From a physical oceanographic point of view, the Puerto Morelos region is characterised by the strong Yucatan Current (YC) flowing offshore, a microtidal environment and a Trade Wind regime (Sheinbaum et al. 2002; Chávez et al. 2003). These physical characteristics in conjunction with the abrupt bathymetry of the region, where depths in excess of 200 m are reached just a few kilometres from shore, imply that an appropriate study must include the monitoring of offshore current patterns in deep water. There have been few studies of the physical processes that take place in the Puerto Morelos reef lagoon. Merino-Ibarra and Otero-Dávalos (1991) made some limited measurements of water current and determined that the circulation in the reef lagoon is mostly parallel to the coast, with an average speed of  $0.1 \text{ m s}^{-1}$ , and a maximum of  $0.5 \text{ m s}^{-1}$  on the inlets that link the lagoon to the open ocean. From this limited information, these authors, and later on Ruíz-Rentería et al. (1998), concluded that currents change in speed and direction due to a combination of variables, including the influence of the YC, winds, wave spillage over the reef, and the location and orientation of inlets. No further information has been made available on the role that each forcing plays on the lagoon, nor has any quantitative estimate been given on the effects these forcing functions have on the ecology of the reef, such as residence times or organic productivity.

The aim of this study was to examine the influence of tides, waves, winds, and the YC on the dynamics of the Puerto Morelos reef lagoon using a recent set of detailed measurements. In particular, the paper examines the spatial and temporal characteristics of each forcing and

their relative contributions to the circulation of the lagoon. Based on the results, a simple model is proposed which uses the observed flow patterns to provide an estimate of the lagoon's water residence time.

## Materials and methods

### Study area

The Puerto Morelos reef lagoon is located on the north-eastern coast of the Yucatan Peninsula, ~25 km south of Cancún. The coast off Puerto Morelos is fringed by a reef that stretches about 4 km in length alongshore, creating a reef lagoon whose width varies between 550 and 1,500 m (Fig. 1). The lagoon is rela-

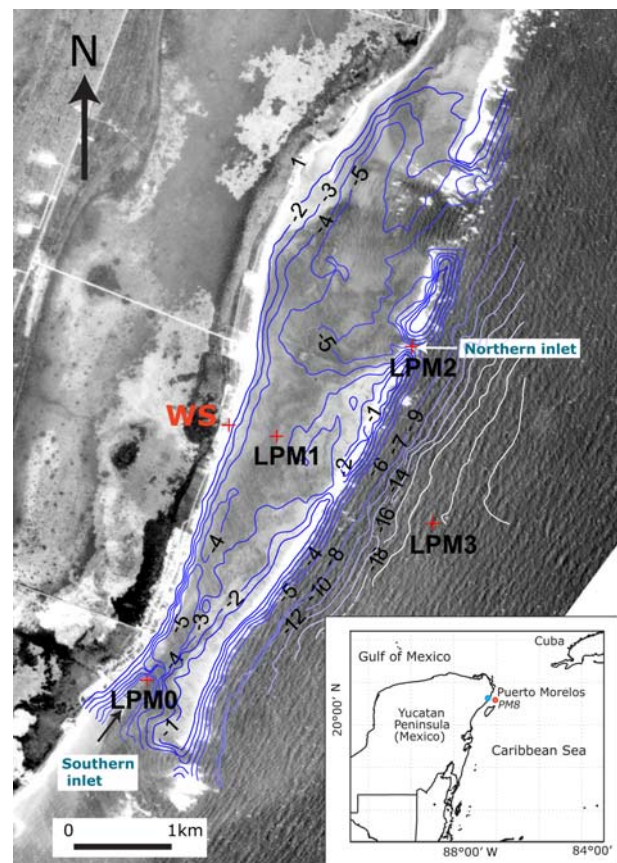


**Fig. 1** Geographical location (inset map) of the study area on the eastern coast of the Yucatan peninsula and aerial photograph of Puerto Morelos showing the morphology of the fringing reef lagoon and the instrument array used in this study. Isobaths are shown in shades of blue and are labelled to each metre of depth. The red crosses indicate the location of the Nortek 1,000 KHz acoustic profilers installed in the reef lagoon, while the WS mark shows the location of the weather station. A deep-water acoustic Doppler current profiler ADCP RDI WorkHorse 300 KHz mooring was located 12 km offshore (indicated with a red dot in the inset map)

tively shallow, with an average depth of 3–4 m and maximum depth of 8 m. It is connected to the open ocean via two inlets: a northern gap in the reef barrier creates an entrance 300 m wide and 6 m deep, whereas a southern 400 m wide navigational channel is dredged to a depth of ~8 m. The bottom of the lagoon is covered by calcareous sand, which is stabilised by seagrass meadows. In certain areas, the underlying calcareous pavement is exposed and colonised by hardground coral reef communities or is covered by unconsolidated carbonate sediments. Seaward from the crest, the reef slopes gently to depths of 20–25 m, giving way to a mostly barren sand platform several kilometres wide. The shelf edge occurs at a depth of 40–60 m, followed by a drop-off to more than 400 m at about 10 km from the reef (Ruíz-Rentería et al. 1998). The reef area is characterised by the presence of shallow, submerged coral banks subjected to significant wave action. Although the region is microtidal, the reefs may be exposed at low-spring tides. Such reefs, surrounding lagoons, provide protection from incident waves by dissipating their energy through the surf zone on the seaward side of the reef.

The climate of the region is tropical, with two dominant seasons defined in terms of wind patterns and air temperature. Winter begins in November, and continues until March or April. Monthly mean air temperature in winter is 24–25°C, but diurnal minima can be substantially lower for brief periods following the passages of cold fronts, locally known as “Nortes”. Monthly resultant wind directions are from the north-eastern quadrant from October to February, although northerly and South-easterly winds occur following the passage of cold fronts. Summer weather patterns are characterised by a dominance of maritime tropical air and frequent thunderstorms. Winds are predominantly easterly Trade Winds with speeds of 3–9 m s<sup>-1</sup>. Maximum air temperature is reached in August, with a monthly average of 29°C and maxima above 33.5°C.

Bottom water temperature in the lagoon has a seasonal variation of about 5°C, ranging from 31 to 32°C on several occasions between mid August and early September, to 24–25°C occurring intermittently between December and mid March.

The wave climate off Puerto Morelos is dominated by swell generated by the Trade Winds blowing over the Caribbean. These waves break on the reef propagating from the east, with an average significant wave height ( $H_S$ ) of 0.8 m and relatively short dominant wave period ( $T_P$ ), typically between 6 and 8 s. However, higher energy waves or “notable” wave events, statistically defined in Puerto Morelos as waves with  $H_S$  higher than 1.75 m, take place 6–8 times each year.

In winter, these weather events are typically a consequence of the passage of cold fronts or “Nortes” over the Gulf of Mexico and the Caribbean Sea. In summer, wave  $H_S$  is usually small ( $H_S < 0.3$  m), but tropical storms or hurricanes temporarily dominate the wave climatology of the Caribbean Sea. Should a hurricane pass through directly over Puerto Morelos, its winds can generate waves of up to 7 m of  $H_S$ , with relatively long periods ( $T_P \approx 10$ –18 s) (unpublished data), and very variable propagation direction due to complex wave patterns generated by the superposition of swell and locally generated sea.

#### Data collection

This study was based on measurements collected between September 2003 and July 2005 using an array of four Nortek 1 MHz Aquadopp acoustic Doppler current profilers (ADCP), mounted on the bottom of Puerto Morelos reef lagoon: one on the centre of the southern inlet at a depth of 8 m (LPM0); the second instrument was installed on the shallow interior of the lagoon, approximately in its centre, in 3.5 m of water (LPM1); the third instrument was deployed at the centre of the lagoon’s northern inlet at a depth of 6 m (LPM2); and the last instrument was installed on the foreereef, 500 m offshore from the barrier and at a depth of 22 m (LPM3). These instruments recorded the current profile each 15 min, along with water temperature and pressure at the instrument head. Surface waves were sampled each hour, collecting bursts of 1,024 samples at 1 Hz. The current metres were exchanged by divers every 3.5 months. Concurrent to this array, a 300 KHz RDInstruments upward looking ADCP was moored in a location 500 m deep, 12 km offshore, within the YC, from August 2003 to August 2004. The ADCPs transducers were positioned at a depth of 130 m, profiling currents from 120 to 23 m every 8 m, with a sampling interval of 30 min. Wind was measured continuously from a fixed platform located at the National Autonomous University of Mexico (UNAM) pier, about 500 m from LPM1 recording site.

## Results

### Circulation patterns

Figure 2 presents a view of the mean and variability ellipses of the surface currents, obtained from 22 months of data. The average circulation consisted of a relatively small current (2–3 cm s<sup>-1</sup>), directed to-

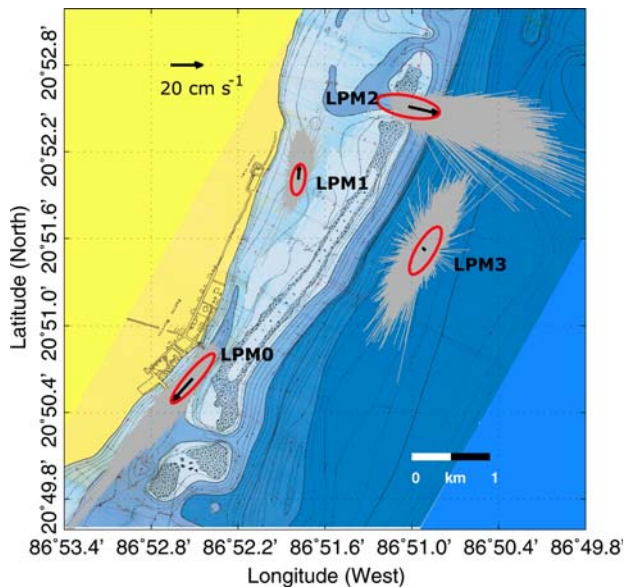


**Fig. 2** Basic statistics of surface current data. The *arrows* show the mean current vector, while the *ellipses* indicate the direction of the mayor and minor semiaxes of variability. The scale of the ellipse represents one standard deviation along each semiaxis. The complete set of surface current data (*grey sticks*) is also shown, each stick representing 1-h average

wards the shore at the forereef station (LPM3). In the northern and southern inlets, the preferential direction of the current was towards the exterior of the lagoon, with an approximate mean speed of  $20 \text{ cm s}^{-1}$ , while inside the lagoon the average current speed was  $10 \text{ cm s}^{-1}$ , directed to the north. The average vertical current profile in LPM0 and LPM2 is almost unidirectional and decreases in magnitude as it approaches the bottom, consistent with a frictional bottom boundary layer. The ellipses show that the average of the current is smaller than its variability, which generally implies frequent reversals of the flow. They also show that, except for the measurements made outside the lagoon, the orientation of the current ellipse is constrained by the inlets (LPM0 and LPM2) or by the orientation of the longitudinal axis of the lagoon (LPM1). Interestingly, the surface current at LPM3 has an average directed cross-shore, but its axis of variability is along-shore. Near the surface, the average current profile is coherent and the current is directed towards the shore, consistent with wave induced drift and Trade winds, which have on average the same direction of the mean current. However, as depth increases, the vectors spiral clockwise down to the bottom. This behaviour is probably the result of a combined effect of bottom friction, the rotation of the Earth, the orientation of the YC and the orientation of tidal currents in the region, which are, in turn, influ-

enced by the bottom topography. In fact, the analysis suggests that at subinertial frequencies (the inertial period at  $20^{\circ}50'$  of latitude is 33.7 h), the variability of the forereef current is dominated by the YC, while at suprainertial frequencies the dominant forcing are the tides.

#### Empirical orthogonal functions analysis

Empirical Orthogonal Functions (EOFs) were applied to the surface current time series in all four locations. However, it was convenient to separate the current signal into its supra- and subinertial components. To achieve this, a lowpass Lanczos filter was designed, with a cut-off frequency equivalent to a period of 48 h. Hence, the highpass of the signal is obtained from the difference between the original time series and its lowpass. It should be borne in mind that since the average was not removed from the current time series, the EOF analysis maximises total energy rather than the variance of the dataset. The result of this analysis for the low-frequency component of the current are shown in Figs. 3 and 4, showing, respectively, the first and second modes of spatial variability; the time series under the map represents the temporal evolution (principal component) of each mode. The first mode (Fig. 3) represents up to 90% of the low-frequency total energy of the surface current, and manifests itself as the average circulation previously described. The positive sign of the temporal evolution of this mode indicates that the circulation is divergent most of the time, with a peak in September of 2004, corresponding to the passage of Hurricane Ivan. Less frequent are the periods in which the sign of the principal component changes. Due to the way in which the EOFs were constructed, a negative value in the temporal evolution of the mode implies a reversal of the vectors, or in this specific setting, the convergence of water in the lagoon. For example, a convergent circulation event occurred in October 2003, albeit the magnitude of the current vectors was so small that it was more appropriately considered as a stagnation of the circulation. These periods of less vigorous circulation are related to low-wave conditions. As it will be further discussed below, this mode explains the main circulation pattern in the lagoon, and is induced by surface waves overtopping the reef.

The second empirical mode (Fig. 4) represents a much smaller proportion of the total energy (7%) and shows currents aligned with the coast with frequent reversals. The most probable explanation of this behaviour is a combined large scale forcing due to wind and the influence of the YC. For example, the October

**Fig. 3** First empirical mode of variability of subinertial surface current. The map shows the spatial structure of the mode. In the time series, below, the principal component (PC) is shown by the *blue trace* along with the significant wave height measured at the foreereef location (*red line*)

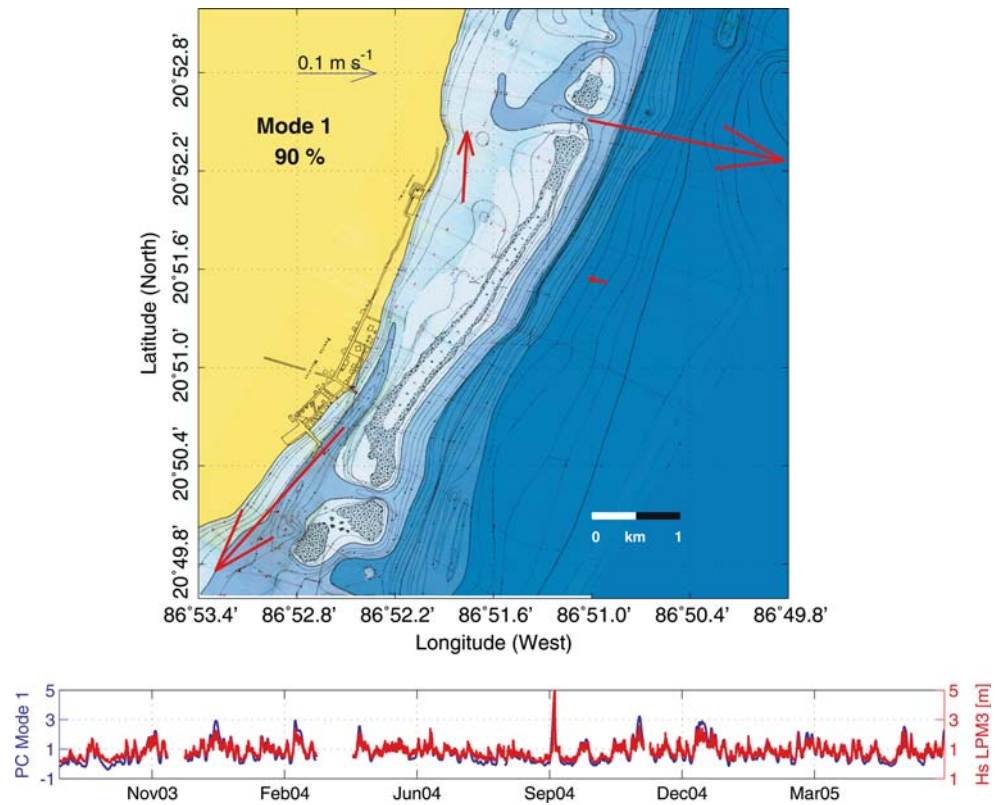
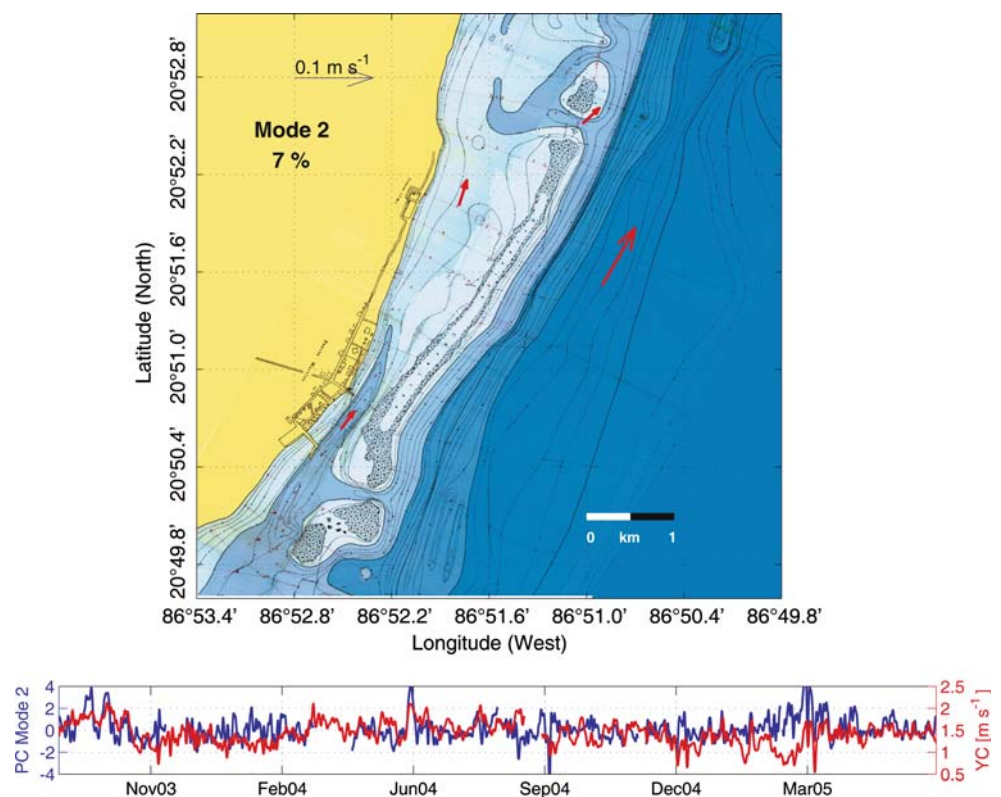


**Fig. 4** Second empirical mode of variability of subinertial surface current. The map shows the spatial structure of the mode, In the time series, below, the principal component (PC) is shown as the *blue trace* along with the Yucatan current principal axis component measured at the offshore mooring (*red line*)



2003 and June 2004 peaks correspond to intensification of the YC. On the other hand, the frequent reversals measured in the winter of 2003–2004 are better correlated to the wind regime, dominated by the “Nortes” and Southeasterlies. The intense reversal shown in September 2004 is most likely a consequence of the passage of Hurricane Ivan. These explanations should, however, be treated with care because of the limited number of simultaneous YC, wind, and lagoon currents measurements.

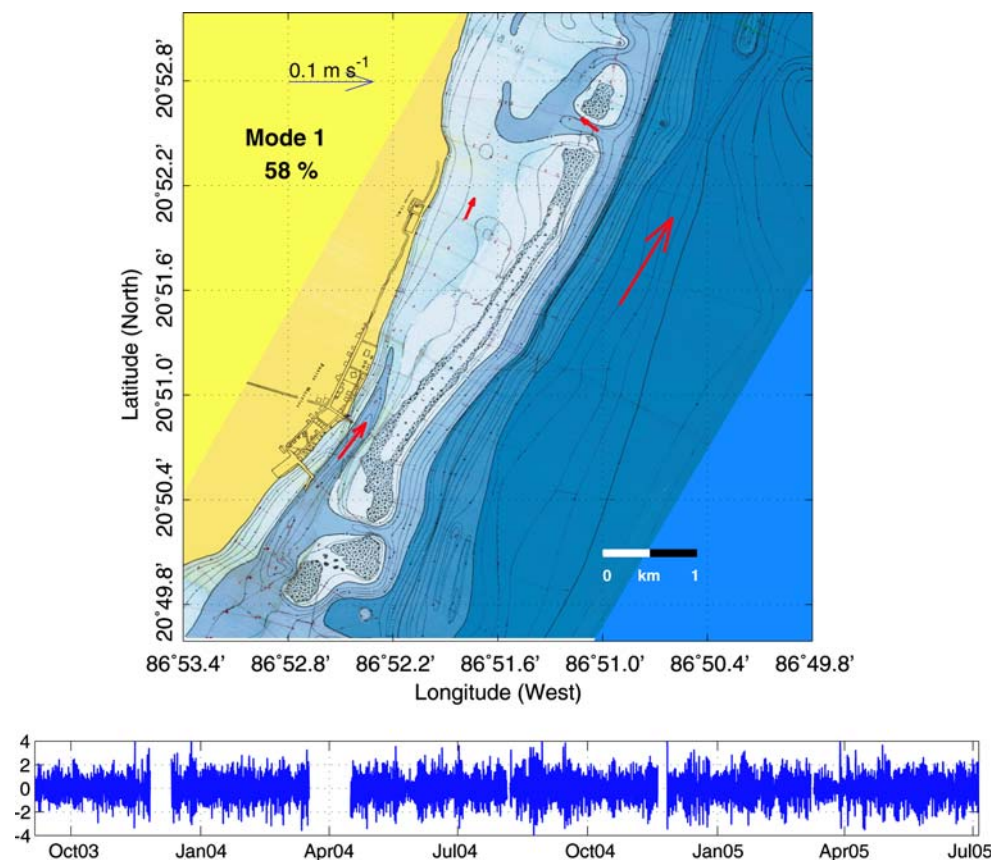
The EOF analysis for suprainertial frequencies is shown in Fig. 5. The first mode, which represents 58% of the high-frequency variability, shows currents aligned with the lagoon’s inlets, directed lagoon-ward during the positive phase of the principal component. At LPM3, the high-frequency current is more intense, and it is oriented parallel to the barrier reef. Harmonic analysis of the temporal variation of this mode reveals that the dominant harmonics are the diurnal  $K_1$  and  $O_1$  constituents, with an amplitude of 0.62 and 0.36, respectively (due to the way in which the EOFs were constructed, the temporal time series has no dimensions, which are contained in the spatial maps). As seen in the next section, this diurnal over semidiurnal dominance in tidal currents is reversed in the tidal sea

level signal, where semidiurnal constituents dominate. The magnitude of the current vector in LPM3 is  $0.12 \text{ m s}^{-1}$ , which explains the intense variability of the observed forereef current, approximately aligned to the barrier reef. Tidal currents are considerably smaller in the inlets of the lagoon. Nevertheless, the orientation of the principal component, with currents converging into the lagoon, implies that during flood the tidal current is opposed to the wave-driven flow (with water flowing seaward regardless of the phase of the tide). Conversely, during ebb tide, the outflowing current is favoured by the tidal currents. Hence, this mode accounts for the tidal modulation of the wave driven flow at the lagoon’s inlets. The physical explanation of the higher modes is unclear, but it can be concluded that at least 58% of the suprainertial variability is due to tidal currents.

#### Effect of changing sea level

The mean tidal range off Puerto Morelos is  $\sim 17$  cm, with a maximum spring tide range of 32 cm and a minimum neap tide range of just under 7 cm. Although all instruments recorded bottom pressure, the measurements are referred to as “sea level” by converting

**Fig. 5** First empirical mode of variability of the suprainertial surface current. The map shows the spatial structure of the mode, while the principal component is shown below the map



pressure into the equivalent water column height. However, they differ from true sea level because they include variations in atmospheric pressure and are therefore compensated for the inverse barometer effect. Harmonic analysis was performed on the sea level measurements of the profilers, using the *t\_tide* program developed by Pawlowicz et al. (2002). Semidiurnal  $M_2$  and  $S_2$  constituents dominate the amplitude of tides at Puerto Morelos. The form of the tides, as determined by the amplitude ratio  $F = (K_1 + O_1)/(S_2 + M_2)$  is 0.34, which describes the tides as mixed, mainly semidiurnal. A comparison among stations reveals that in the interior of the lagoon the amplitude of the harmonics increases relative to LPM3, except for the diurnal  $K_1$ . Likewise, the phase of all harmonics is similar, although the tide at LPM1 is consistently lagged with respect to LPM3, e.g. the delay of the tide between the lagoon and the adjacent ocean for the semidiurnal  $M_2$  component is 1 min.

The importance of tidal currents can be estimated through harmonic analysis of the measured currents and by calculating the percentage of variance that tides can explain. In the Southern and Northern inlets (LPM0 and LPM2), tidal currents account for less than 10% of the variance of the current along the principal axis. However, on the forereef, (LPM3) tidal currents can explain up to 25% of the observed variability. This result is consistent with the high-frequency EOF analysis, which revealed an increased magnitude of tidal currents outside the lagoon. Hence, tides have a minor role on the dynamics of the lagoon's interior, but are relatively important for the current regime on the forereef. It is interesting to note that the harmonic analysis reveals a slight annual modulation in the current pattern. Certainly, this is not of astronomic origin but is rather associated with the annual cycle of the wave climatology in this region, implying that during winter, when the significant wave height is on average higher, the overall transport is increased.

Another interesting feature revealed by the sea level measurements is the large difference between measurements and the astronomic tide. This is illustrated in Fig. 6: panel (a) shows 22 months of hourly sea level measurements in the interior of the lagoon (LPM1), whilst panel (b) shows the tidal prediction, using all relevant harmonics, along with the residual (observations minus prediction). It is evident that the residual has amplitudes sometimes larger than the astronomic tide itself. The sea level rise observed on September 2004 can be attributed to the passage of Hurricane Ivan, but the origin of the remainder of the variability requires an explanation. The amplitude spectra (c) indicates that the most important components of sea

level change are within the semidiurnal band, but amplitudes comparable to the diurnal tide can be observed from the fortnightly to the 6-month bands. However, it can be demonstrated that the forcing causing these oscillations has neither constant amplitude nor constant phase, which implies that their origin is not astronomical. A first candidate to explain this variability might be the wind stress, which according to its direction could rise or lower the sea level. The second candidate is the variability of the strong YC, which is discussed in the next section.

### Influence of Yucatan Current

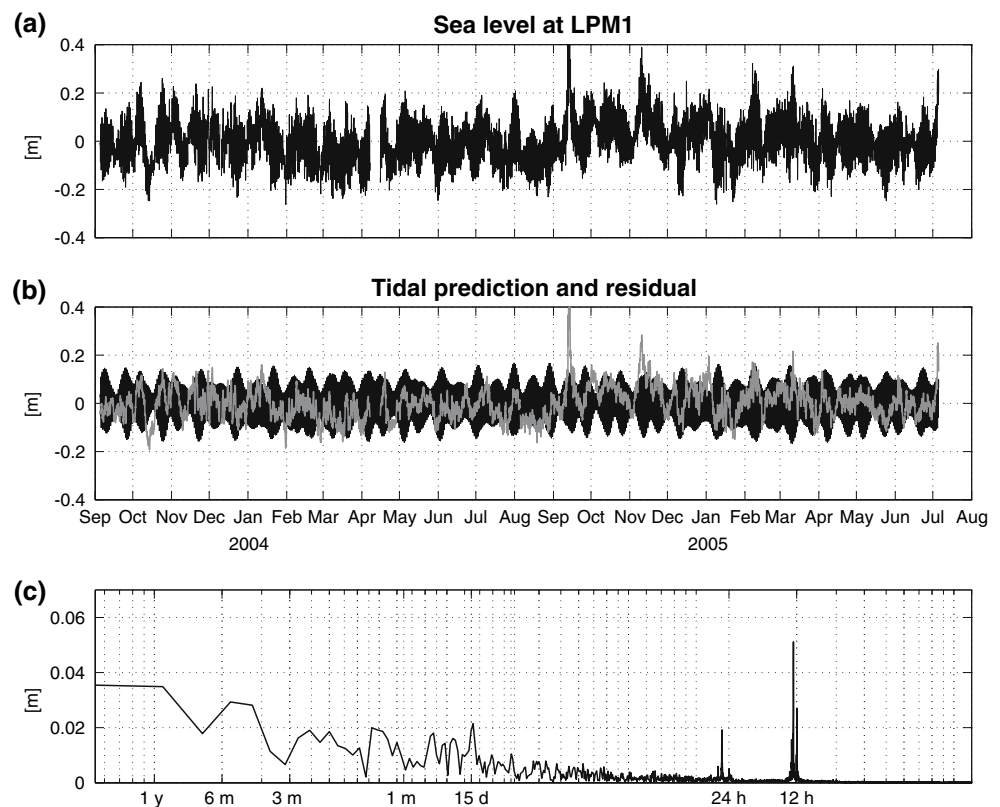
The influence of the YC is first characterised by describing the basic statistics of the current measurements obtained from mooring PM8, ~12 km offshore from Puerto Morelos, deployed in the core of the YC. Panel a of Fig. 7 shows that the mean current vector is  $1.5 \text{ m s}^{-1}$ , towards the Northeast. Panel b shows the temporal behaviour of the uppermost measured current bin (30 m deep), along and across its principal current axis. The annual variability cycle of the YC is evident, with more intense currents (up to  $2 \text{ m s}^{-1}$ ) from April to November, while during the winter its intensity decreases to a minimum of  $0.9 \text{ m s}^{-1}$ . This scenario is consistent with previous analysis on the YC (see for example Chávez et al. 2003, and the review of Badán et al. 2005).

One way to determine the possible influence of the YC on the nearshore circulation is by comparing the observed current at LPM3 with those at the deep-water mooring (PM8). The vector component scatterplot (Fig. 8) shows that even though in both locations the orientation of the principal variability axis is similar, the nearshore current has a significantly smaller magnitude than the YC. Moreover, the surface current at LPM3 shows frequent reversals, something never observed in the YC (Chávez et al. 2003). Clearly, LPM3 is within the lateral boundary layer of the YC. Other possible coupling mechanisms are the pressure gradient and the sea level change induced by the geostrophic adjustment of the YC, which will be discussed in the following section.

### Geostrophic balance

Since the mean and principal axes of the YC are oriented towards the Northeast at PM8, this orientation was chosen as the natural reference to study the YC variability. In this new reference frame, the *y*-axis is along the axis of maximum kinetic energy, while the *x*-axis is perpendicular to this direction and to the coast

**Fig. 6** **a** Relative observed sea level at LPM1. **b** Sea level tidal prediction (*black trace*) with the residual observation-prediction (*grey line*). **c** Amplitude spectrum of the sea level record shown in **(a)**. The units in the vertical axis are metres, and the horizontal axis is period, logarithmically scaled



orientation, approximately to the Southeast. Considering that the YC is in geostrophic balance in the across shelf direction, gives

$$fv = \frac{1}{\rho_o} \frac{\partial P}{\partial x}, \quad (1)$$

where  $v$  is the velocity component along the  $y$ -axis,  $f$  is the Coriolis parameter,  $P$  is the pressure and  $\rho_o$  is a reference density. Furthermore, assuming hydrostatic balance in the vertical, i.e.  $P = \rho_o g \eta$ , yield

$$\Delta \eta_G = \frac{fv \Delta x}{g}, \quad (2)$$

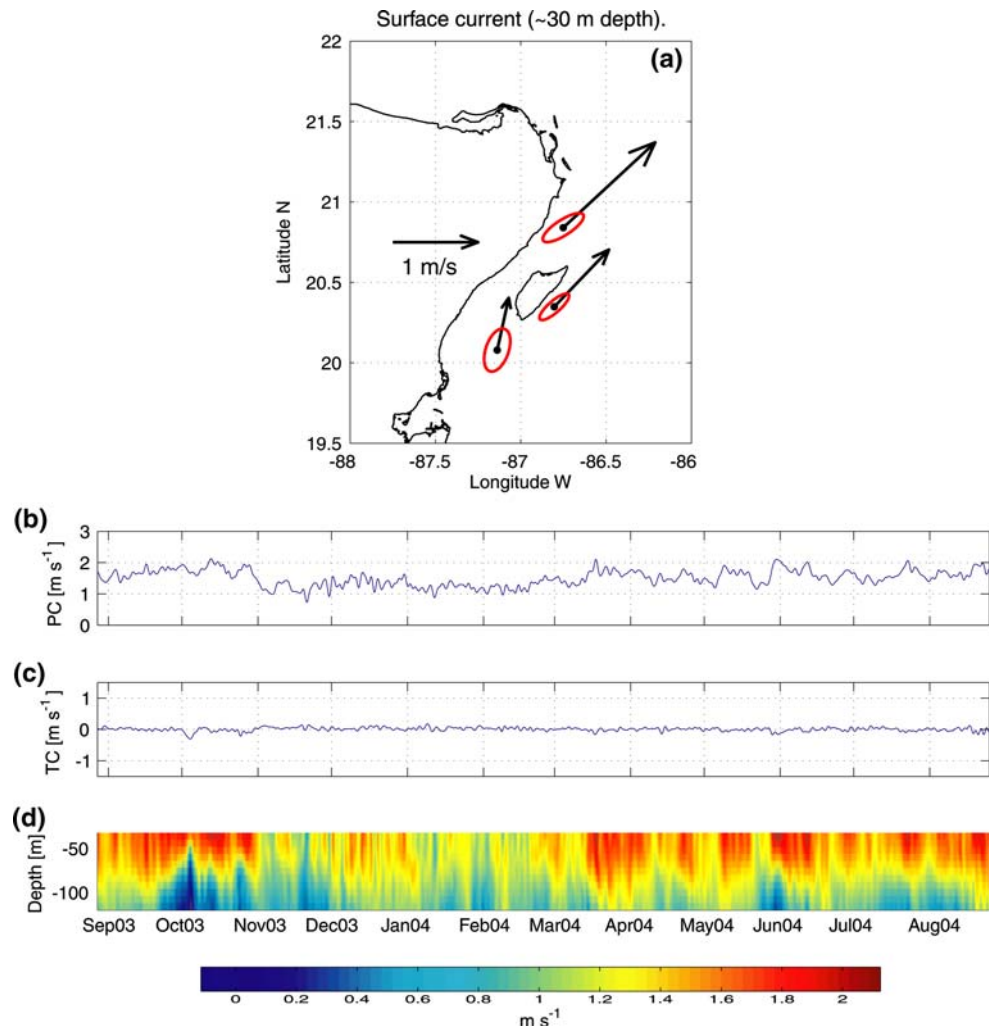
which relates the sea level difference  $\Delta \eta_G$  across the current with its magnitude in the along-current direction at the surface. Equation 1 in the reference frame of the study area implies that since  $\partial P / \partial x$  is positive, the geostrophic adjustment of a current directed towards the positive  $y$ -axis results in a lower sea level inshore than offshore. At the same time, since  $v$  is proportional to  $\partial P / \partial x$ , the fluctuations of the magnitude of the YC influences the sea level at Puerto Morelos station. In particular, an intensification of the current implies a generalised lowering of sea level at the coast, assuming that the offshore sea level does not change. Thus, the

validity of this hypothesis could be verified if the intensification of the YC matches with periods of generalised descent of the sea level. Figure 9 provides evidence that the variability of the YC is responsible for a large fraction of the non-astronomic, subinertial changes of the sea level. The most important event of sea level descent matches with the period of highest observed magnitude of the YC, on about 12 October 2003. The correlation between the two series in Fig. 9 is  $r = -0.42$  (small but significant,  $p < 0.05$ ), and for the total series (about a year-long from August 2003 to August 2004) the correlation increases slightly to  $r = -0.49$ .

#### Wind influence

On average, the wind at Puerto Morelos blows from the East, revealing a constant influence of the Trade winds. However, from November to March several intense events were measured, which can be correlated with the passage of cold fronts over the Gulf of Mexico (“Nortes”). These events were characterised by a pronounced drop in atmospheric pressure, air temperature, and relative humidity. When “Norte” conditions prevail, wind blows from the Southeast, with speeds of about  $10 \text{ m s}^{-1}$ ; over a period of days, the wind gradually veers until it is blowing from the North.

**Fig. 7** **a** Basic statistics of the Yucatan Current measurements. The arrow represents the average current vector, and the ellipses are scaled to one standard deviation. Two other measurement locations are shown for reference only. **b** Principal axis component of the current (*PC*). **c** Transversal component (*TC*) of the surface current in PM8. **d** Temporal variability of the vertical profile of the current, projected along the principal component



Fourteen of these events were registered during the winter of 2003, but only six resulted in sustained wind speeds over  $10 \text{ m s}^{-1}$ . These wind events can temporarily drive the low-frequency component of the circulation in the lagoon and in the forereef, as suggested in Fig. 4. Taking more than a year of measurements, the maximum correlation found between wind and subinertial currents in the interior (LPM1) was  $r = 0.52$  for wind blowing from the Southeast, whilst at the forereef (LPM3) the wind and subinertial currents showed a maximum correlation of  $r = 0.43$  for wind blowing from the Southwest. These correlations, albeit significant, are rather small and indicate that the most efficient mechanism for wind influence is through the generation of wind waves, rather than a direct frictional coupling.

#### Surface waves influence

The analysis of transport between the lagoon and the ocean ( $Q_1$ ) together with current's principal compo-

nent analyses support the hypothesis that waves are the main forcing of the reef lagoon circulation. In fact, as Fig. 3 shows, there is a high correlation between the temporal evolution of the subinertial first EOF mode and the significant wave height at LPM3 ( $r = 0.9$ ). This justifies a more detailed examination of surface wave processes.

It is evident that wave height in the interior of the lagoon (LPM0 and LPM1) is reduced because waves have already dissipated over the reef: the average  $H_S$  at LPM0 was 0.15 and 0.3 m at LPM1, with maxima of 0.69 and 1.33 m, respectively. In contrast, northern inlet (LPM2) and forereef (LPM3) sensors detected higher values of  $H_S$ : 0.63 and 0.83 m on average as well as 2.5 and 5.7 m maxima, respectively. All maxima were recorded during the passage of Hurricane Ivan in September 2004.

During the second measurement period, the instruments at LPM0 and LPM2 gathered no wave data; hence, the following discussion considers only the data at LPM3. Waves at this location normally have signif-

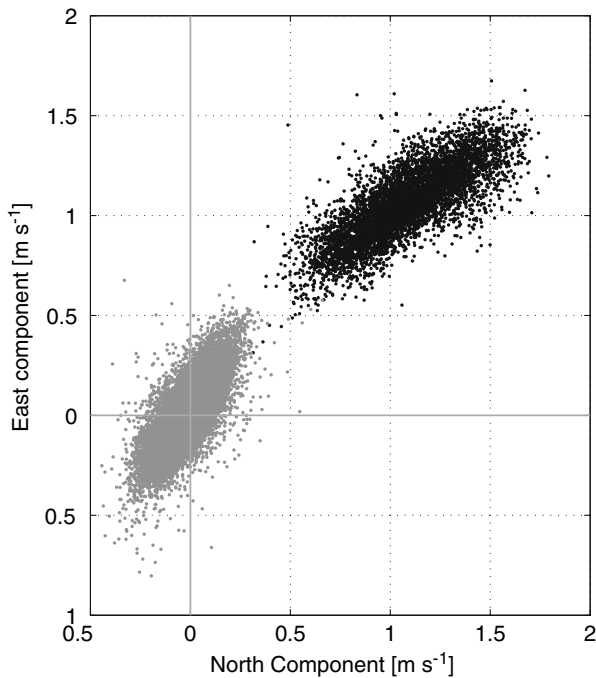


**Fig. 8** Component ( $u$ ,  $v$ ) scatterplot, comparing the surface current measurements at LPM3 (grey dots) and at PM8 (black dots)

icant wave heights ( $H_S$ ) of 0.5–1.5 m, and relatively short dominant wave period ( $T_P$ ), typically between 6 and 8 s. Such a relatively low-energy wave regime can include the influence of higher energy waves or “outstanding” events. Typically, 6–8 of these events take place each year. In winter, the passage of cold fronts or “Nortes” induces waves with  $H_S \approx 1.5$ –2.5 m and  $T_P \approx 4$ –8 s, arriving from the northeast; in summer,

wave heights are fairly small and very calm conditions that last for weeks are not uncommon. It is nonetheless during the summer when record wave heights have been measured, due to the passage of hurricanes.

At this juncture, it is useful to define a quantitative measure to establish a separation between normal conditions and outstanding (or extreme) wave events. The criteria for this separation are based upon a confidence interval, defined by the average of  $H_S$  measurements plus two standard deviations, thus enclosing 95% of the measurements. Consequently, any wave event in Puerto Morelos that exceeds a  $H_S$  of 1.75 m is considered outstanding. Figure 10 shows time series of  $H_S$  at LPM3 together with the direction and period of the most energetic waves. The red line in panel (a) represents the mean plus two standard deviations. Between September 2003 and July 2005, 12 outstanding events were measured, evenly distributed along this period. However, the particular characteristics of winter extreme events were somewhat different from those in summer. For example, the event measured at the beginning of March 2004 lasted  $\sim 1$  week, with a maximum  $H_S$  of 2 m, whilst its wave period was relatively short (6–7 s). The most revealing characteristic was the behaviour of the direction of propagation of the waves: before the event, waves arrived from the East, which is the average direction throughout the year; during the event, waves started to arrive from the Southeast, slowly turning during the course of a week to finally arrive from the Northeast. This is a consistent description of waves that would be induced by the “Nortes”, namely with the waves aligning with the direction of the dominant wind, albeit due to the configuration of the

**Fig. 9** Comparison between the principal component of the Yucatan Current (black line, left hand y-axis) and the relative sea level (grey line, right hand y-axis) at LPM3. Both series were low-pass filtered, with a cut-off frequency equivalent to 48 h

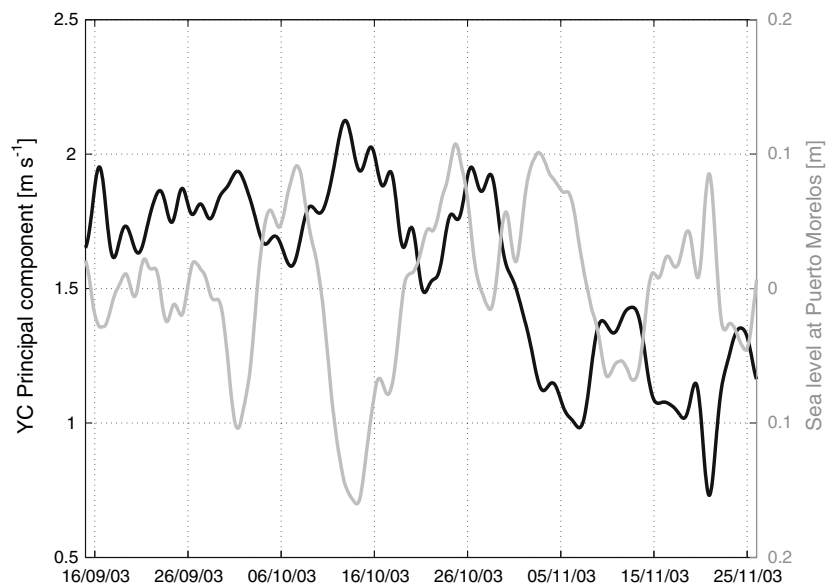
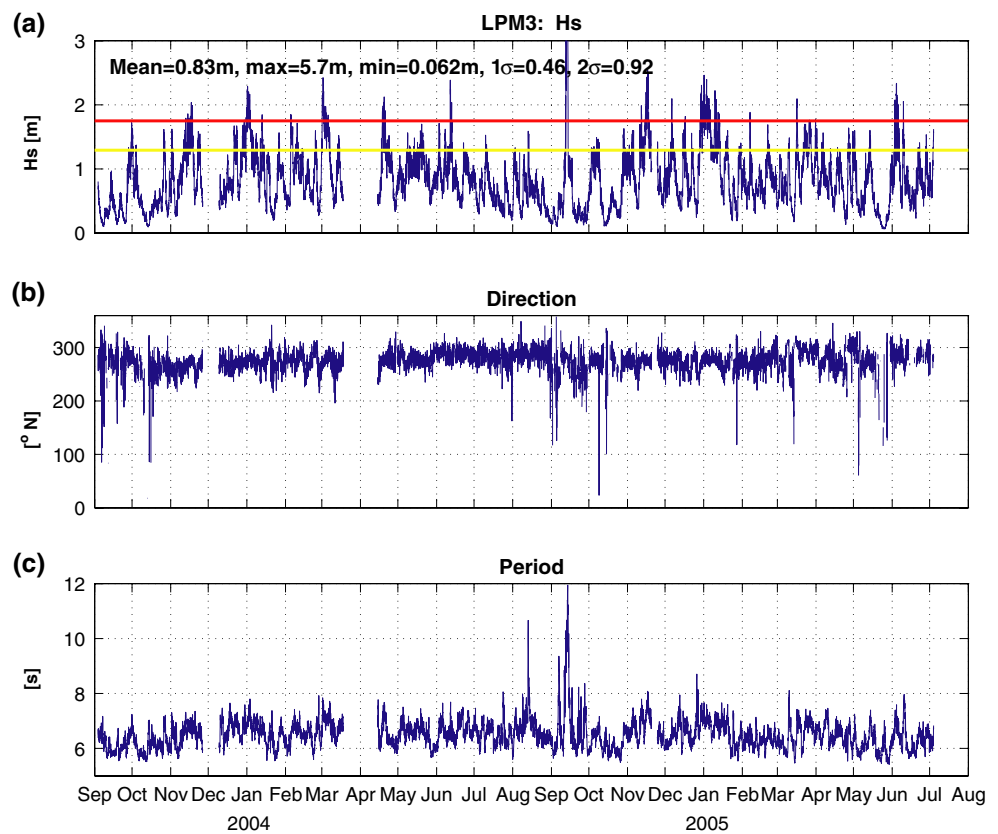


**Fig. 10** Integral parameters of the wave measurements at LPM3. **a** Basic statistics of  $H_S$  information. The *yellow line* indicates the value of the mean plus one standard deviation, and the *red line* indicates the mean plus two standard deviations. **b** Peak wave direction, oceanographic convention; **c** peak period



coast and refraction the waves finally arrive from the Northeast.

During the summer, the wave conditions are much calmer, and extended calm periods ( $H_S < 0.1$  m) that last over a week are common. Despite this, it is during the summer when the largest waves have been recorded. For example, the extreme event of September of 2004 is a result of the passage of Hurricane Ivan through the area. At that time, the maximum  $H_S$  was 5.7 m and the peak period was relatively long ( $>12$  s). Other long-period swell arriving at Puerto Morelos was related to the passage of hurricanes Bonnie, Charley, and Earl. These storms travelled through the Caribbean Sea, from the Lesser Antilles to the Yucatan Channel and on to Cuba, and in the course of this passage they generated waves over a relatively large fetch.

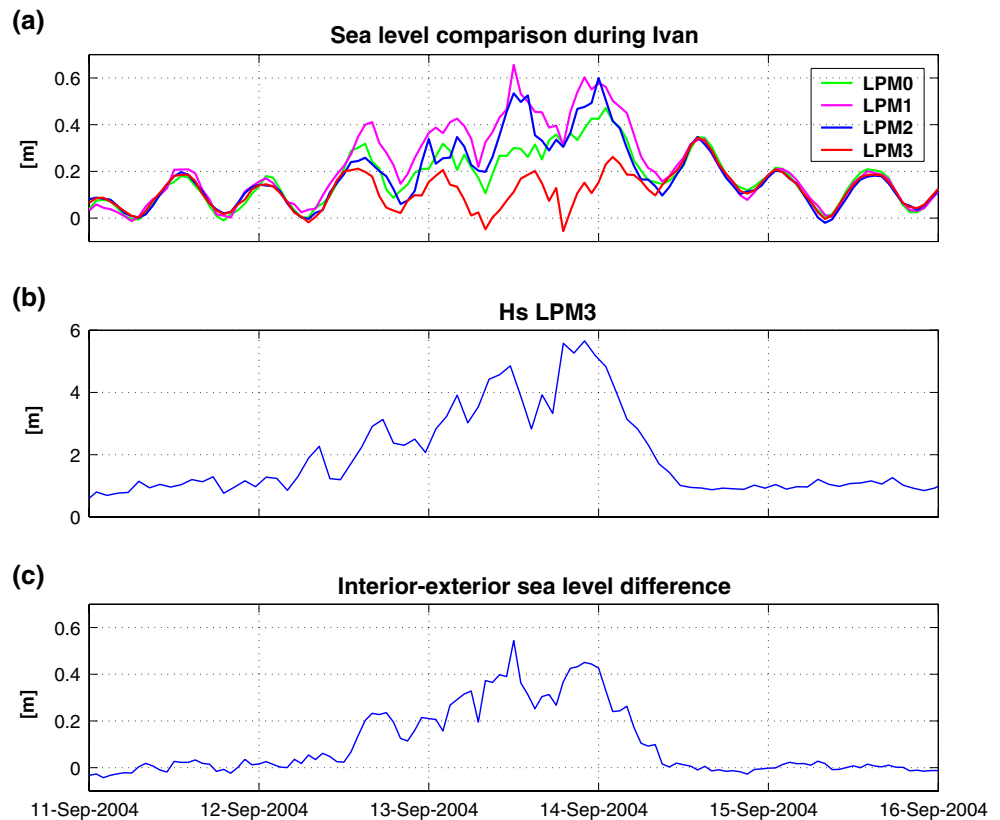
The main effects of a hurricane passing across the shoreline are the generation of strong wind-induced currents, sea surface temperature cooling, and setup which represents an accumulation of water on the shore due to breaking waves and wind drag giving rise to higher local sea level. Figure 11 shows evidence of this sea level rise as a consequence of Hurricane Ivan. Before the hurricane,  $H_S$  averaged 1 m, and the sea level difference between the interior and the exterior

of the lagoon was minimal. Wave heights increased on 12 September 2004 and reached an  $H_S$  maximum of 5.7 m; simultaneously, the relative sea level in the interior of the lagoon rose, whilst remaining stable on the seaward side. Station LPM1 showed the highest storm setup with a sea level difference of 0.55 m between the lagoon and the open sea. The sea level difference was smaller at LPM2, while at LPM0 it was just 0.2 m. This difference in sea level of 0.55 m between LPM1 and LPM3 occurs over a horizontal distance of just 1,800 m. Apart from these extreme hurricane conditions, a positive sea level difference between LPM1 and LPM3 also occurs during normal wave conditions. As discussed later, it is this induced wave setup that is responsible for driving the currents at the lagoon inlets.

#### Water residence time in the lagoon

Several authors have suggested various methods for the determination of water residence timescales, which may be applied to the Puerto Morelos reef lagoon (e.g. Gallagher et al. 1971; Deleersnijder et al. 1997; Tartinville et al. 1997; Andréfouet et al. 2001). Before proceeding, it is necessary to give precise definitions of residence time and turnover time. According to

**Fig. 11** Pressure gradient induced by setup of Hurricane Ivan swell. **a** Comparison between sea level measurements at the four locations. **b**  $H_S$  time series at LPM3 during Hurricane Ivan. **c** Difference between the sea level at LPM1 and LPM3



Tartinville et al. (1997), “the residence time ( $T_r$ ) at a given point in the lagoon is the period of time that a water parcel, initially located at the point considered, needs to leave the lagoon” through its connections with the open ocean. The turnover time  $T_t$  is obtained by averaging the residence time over the volume of the lagoon.  $T_t$  is relevant on a lagoon-wide scale and it is spatially independent, whereas  $T_r$  is explicitly location-dependant. It is worth emphasising that neither  $T_r$  nor  $T_t$  can be determined on the basis of simple physical reasoning alone.  $T_r$  and  $T_t$  can only be determined by particle tracking or numerical simulation. Nonetheless, a lower bound value for  $T_t$  can be estimated from the ratio of the volume of the lagoon ( $V$ , obtained through bathymetric surveys) to the lagoonal transport ( $Q_L$ ),

$$T_t = \frac{V}{Q_L}. \quad (3)$$

Using the current measurements at the lagoon inlets, an estimate of the transport flowing through each of the inlets can be obtained. The sum of these transports is the total lagoonal transport  $Q_L$ . A suitable value for  $V$  is about  $8,000,000 \text{ m}^3$ , and the mean lagoonal transport  $Q_L$  is  $986 \text{ m}^3 \text{ s}^{-1}$ . Using these values in Eq. 3, an average value of  $T_t = 2.25 \text{ h}$  was obtained (Fig. 12). However, during calm wave conditions

( $H_S < 0.1 \text{ m}$ ),  $Q_L$  may be zero or change its sign. Since Eq. 3 tends to infinity as  $Q_L$  approaches zero, the practical interpretation of the turnover time analysis is that the residence time will increase dramatically whilst wave conditions remain calm, which from the observations in this study can be up to 2 weeks. These calm conditions are most likely to occur during the summer when local factors (prolonged periods of low waves, low wind, and a sea level decrease related to the intensification of the YC), rather than large scale meteorological factors are dominant. Conversely, during extreme wave weather, e.g. swell caused by Hurricane Ivan, the turnover time decreased to the lower bound value of  $T_t = 0.35 \text{ h}$ .

These values are in agreement with the results of other studies in similar physical settings. For example, during the TypAtoll project, Pages and Andréfouet (2001) found that  $T_t = 7.2 \text{ h}$  in Tekokota lagoon, an atoll with an area of  $5.11 \text{ km}^2$ , average depth of  $3 \text{ m}$  and a volume of  $0.015 \text{ km}^3$ .

## Discussion

At Puerto Morelos, the average flow scenario establishes the general patterns of the circulation in the reef lagoon. In the northern and southern inlets, the

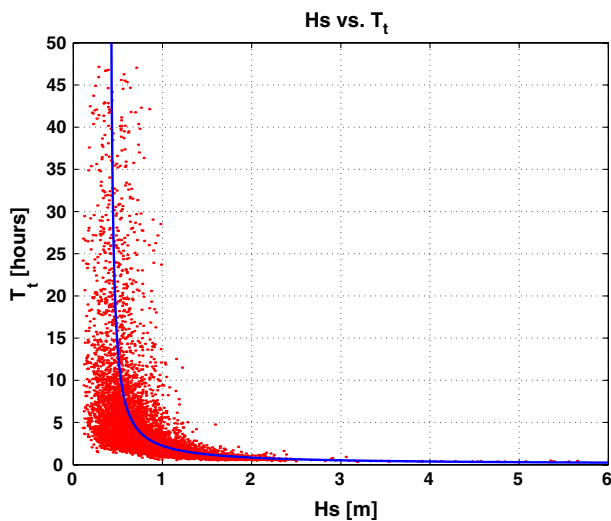


**Fig. 12** Relationship between  $H_S$  and the turnover time  $T_t$ . The red dots indicate the measurements whereas the blue line shows the best fit according a relationship  $T_t$  proportional to  $(H_S)^{-1}$

asymmetry of the current favours a flow directed to the exterior of the lagoon, with a maximum magnitude of  $1.5 \text{ m s}^{-1}$  during strong meteorological events (e.g. hurricanes). Currents in the interior of the lagoon are also asymmetrical, though to a lesser extent, such that the main direction of the current was to the North, whereas the maximum measured current ( $0.6 \text{ m s}^{-1}$ ) was towards the South southeast. In contrast, the surface current on the forereef showed a tendency to be symmetrical, and rarely exceeded  $0.5 \text{ m s}^{-1}$ . The main forcing of the circulation in the interior of the lagoon and its inlets clearly induces a unidirectional flow, regardless of the phase of the tide. Other studies in lagoons with similar size and oceanographic setting have concluded that the factor responsible for this behaviour is the cross-reef flow induced by the breaking of the waves on the barrier reef (Tait 1972; Young 1989; Symonds et al. 1995; Kraines et al. 1998; Hearn 1999; Storlazzi et al. 2004).

The analysis of the average current suggests a conceptual model for the mean circulation in the Puerto Morelos reef lagoon (Fig. 13). Surface waves breaking over the reef crest generate a unidirectional water flow ( $U_R$ ) towards the interior of the lagoon, which is dependant on the significant wave height ( $H_S$ ) and the relative sea level ( $h$ ) at the forereef. This wave induced flow accumulates water in the lagoon, raising its level and causing the excess water to leave through the inlets, where the currents are driven by the sea level difference between the lagoon and the adjacent ocean. In general, the current velocity in the interior of the lagoon ( $U_L$ ) should be the result of the sum of the current induced by all the forcing terms: reef current

induced by waves ( $U_R$ ), tidal currents ( $U_T$ ), wind generated currents ( $U_W$ ), and the current induced by the YC ( $U_{YC}$ ), though the latter may be an indirect influence through modulation of  $U_R$ .

If the analogies are established between this simplified model and the experimental setting of Puerto Morelos, it can be seen that the measurements of wave height and relative sea level allow an approximate value for the reef current to be determined. The volume balance in the lagoon indicates that this water must have entered over the barrier reef and consequently be correlated with the incident waves. Indeed, the comparison between  $Q_L$  and  $H_S$  has a significant correlation of  $r = 0.89$ , which indicates that most of the transport variability may be explained by surface waves. This simplified description can be framed as a statistical model that can be validated using multiple regression analysis, through least squares fitting. The objective is to obtain a quantitative estimate of the relative importance of each of the studied forcing functions. The statistical model can be expressed as:

$$Q_L = aH_S + bT + cW + dY, \quad (4)$$

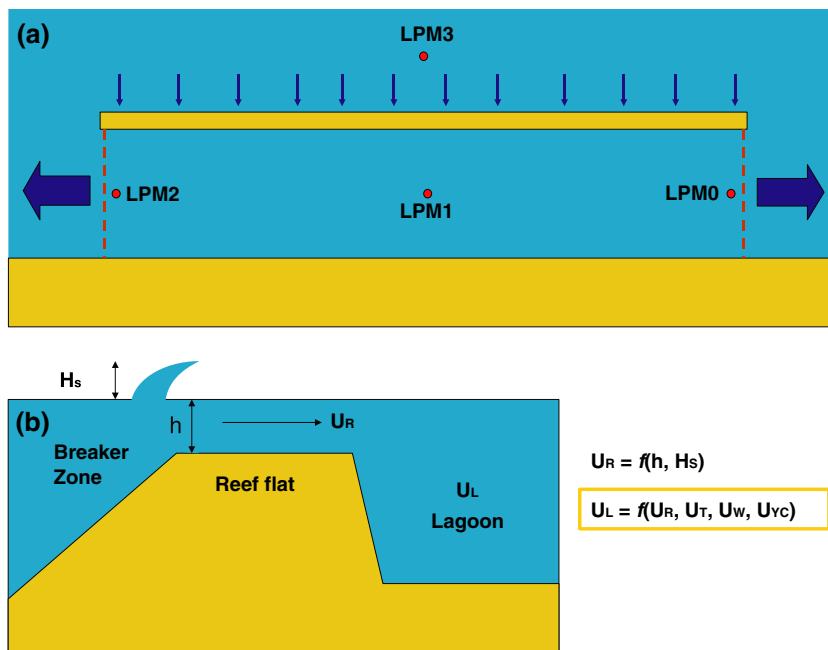
where  $H_S$ ,  $T$ ,  $W$  and  $Y$  (wave  $H_S$ , tide, wind and YC, respectively) are the simultaneous time series of wave  $H_S$  at LPM3, tide prediction at LPM1, wind along the lagoon's principal axis (Northeast) from the weather station at the UNAM pier and the current's principal component measured at PM8, respectively; the coefficients  $a$ ,  $b$ ,  $c$  and  $d$  represent the relative importance of each forcing. To obtain an unbiased fit, each time series was detrended and normalised by its standard deviation. The model thus constructed has non-dimensional coefficients with values between 0 and 1, and for a perfect fit  $|a| + |b| + |c| + |d| = 1$  should hold true.

The fit between the model and the measurements is relatively good with an  $r = 0.91$ . However, the most interesting result is the value for the coefficients:  $a = 0.87$ ,  $b = -0.024$ ,  $c = -0.018$ , and  $d = -0.14$ . The value for  $a$  implies that waves contribute 87% of the variability of the lagoonal transport, which is consistent with the previous discussion. Likewise, the value of  $d$ , corresponding to the relative influence of the YC, indicates that it contributes markedly to the variability of the dynamics of the lagoon, but has a negative effect: the greater YCs intensity, the less vigorous the transport is in the lagoon. The explanation of this behaviour is that since the YC modulates the sea level in Puerto Morelos through geostrophic coupling, its intensification causes the dominant forcing, waves, to become less efficient. In fact, as the sea level decreases, the surf zone moves away from the reef barrier, subjecting the

**Fig. 13** Conceptual model of the circulation in Puerto Morelos reef lagoon.

**a** Idealised configuration of the reef, along with the location of measurement stations (LPM0 to 3). The arrows show the conceptualisation of the measured flows.

**b** A transversal cut through the reef.  $H_s$  significant wave height,  $h$  sea level height,  $U_R$  wave-induced cross reef current, as a function of  $H_s$  and  $h$ ,  $U_L$  lagoonal current,  $U_T$  tidal current,  $U_W$  wind-induced current,  $U_{YC}$  Yucatan Current effect



reef current to greater dissipation across the increased distance over the reef. Finally, the values for  $b$  and  $c$  suggest that the overall contribution of tides and wind in the long-term circulation is small.

Together with this average circulation model, the behaviour of the circulation under extreme weather conditions defines the description of the physical processes in this reef system. For example, during Hurricane Ivan, the water accumulation in the interior of the lagoon was a consequence of the increased reef current due to the large swell. This accumulation imposed a pressure gradient between the interior and the exterior of the lagoon, and to sustain this large pressure gradient the lagoonal current must be in balance with bottom friction (Hearn et al. 2001). This kind of balance is common in shallow water, but coral reefs are unusual with respect to the magnitude of the surface slope they can support through frictional stress at their connecting inlets. To calculate a value for the friction coefficient, a balance between the pressure gradient and a linear friction model can be considered:

$$0 = -\frac{1}{\rho} \frac{\partial P}{\partial x} - \lambda u, \tag{5}$$

where  $\lambda$  is a decaying timescale that can be interpreted as  $\lambda = C_d U / h$ , where  $C_d$  is a non-dimensional friction coefficient,  $U$  is a characteristic current velocity and  $h$  is depth. Substitution of a vertical hydrostatic balance in (5) and giving discrete values of  $\Delta\eta$  and  $\Delta x$  yields

$$C_d = \frac{gh \Delta\eta}{U^2 \Delta x}. \tag{6}$$

Considering hurricane maximum current velocity  $U$  of order  $1 \text{ m s}^{-1}$ , a sea level difference  $\Delta\eta$  between the interior and the exterior of the lagoon of  $0.55 \text{ m}$ , a separation between measurement locations  $\Delta x$  of  $1,800 \text{ m}$ , and an average depth  $h$  of  $5 \text{ m}$ , Eq. 4 provides a  $C_d = 0.015$ . This number is consistent with the value of  $C_d = 0.02$  obtained by Wolanski (1983) on the Great Barrier Reef, and within the order of magnitude of  $C_d = 0.06$  calculated by Lugo-Fernández et al. (1998) for the Tague reef, Virgin Islands (USA). The value reported here is considerably larger than the one commonly used in sand basins ( $C_d = 0.0025$ ), revealing the extreme roughness of corals.

The description of the hydrodynamics of the Puerto Morelos reef lagoon has been possible thanks to a unique dataset, which up to date represents the most detailed study of the physical oceanography of a coral reef system in the Caribbean. The separation of processes as low- and high-frequency components provides a crisp image of the temporal and spatial scales relevant to the general circulation of the water in the lagoon. Tides, both in currents and sea level variability, play a minor role on the lagoon’s circulation due to the microtidal regime characteristic of the region. On subinertial frequencies, the dominant forcing term is a surface wave induced water flux across the reef. This is clearly achieved through a non-linear process that converts suprainertial surface wave energy into a sub-

inertial flow signal. The wind contributes through the swell generated by the Trade Winds over the Caribbean fetch that in turn reaches the lagoon. Also, during the “Nortes” and Southeasterlies wind events, short-term circulation patterns are set up within the lagoon; however, these are commonly masked by the surface wave induced flows. The YC has an indirect effect on the circulation by modulating sea level in front of the lagoon, thus affecting the efficiency of the surface wave induced flows. However, since Puerto Morelos lies on the lateral boundary layer of the YC, a direct coupling cannot be discarded and should be studied in more detail.

**Acknowledgments** The authors wish to thank Sergio Ramos, Edgar Escalante, and Francisco Ruíz for their enthusiastic contribution on the field work. We also thank the captain and crew of the B/O Justo Sierra, and the technical staff that works on CICESE’s CANEK programme (Ignacio González, Armando Ledo, Carlos Flores, Joaquín García, Miguel Ojeda and Benjamín Pérez). Thanks are also due to Dr. Antoine Badán for critically reading our manuscript. Cesar Coronado was funded by CONACYT, the Departamento de Oceanografía Física of CICESE, and the Instituto de Ciencias del Mar y Limnología (UNAM) through the Global Environmental Facility-World Bank Coral Reef Targeted Research and Building Capacity for Management programme, of which this paper is a contribution.

## References

- Andréfouet S, Pagés J, Tartinville B (2001) Water renewal time for classification of atoll lagoons in the Tuamotu Archipelago (French Polynesia). *Coral Reefs* 20:399–408
- Atkinson M, Smith SV, Stroup ED (1981) Circulation in Enewetak atoll lagoon. *Limnol Oceanogr* 26:1074–1083
- Badán A, Candela J, Sheinbaum J, Ochoa J (2005) Upper-layer circulation in the approaches to Yucatan channel. In: Sturges WS, Lugo-Fernández A (eds) *Circulation in the Gulf of Mexico: observations and models*. Geophysical Monograph Series 161 American Geophysical Union, Washington, DC, pp 57–69
- Chávez G, Candela J, Ochoa J (2003) Subinertial flows and transports in Cozumel Channel. *J Geophys Res* 108:1901–1911
- Deleersnijder E, Tartinville B, Rancher J (1997) A simple model of the tracer flux from the Mururoa Lagoon to the Pacific. *Appl Math Lett* 10:13–17
- Gallagher BS, Shimada KM, Gonzalez FI, Stroup ED (1971) Tides and currents in Fanning atoll lagoon. *Pac Sci* 25:191–205
- Hearn CJ (1999) Wave-breaking hydrodynamics within coral reef systems and the effect of changing relative sea level. *J Geophys Res* 104:30007–30019
- Hearn CJ, Atkinson MJ, Falter JL (2001) A physical derivation of nutrient-uptake rates in coral reefs: effects of roughness and waves. *Coral Reefs* 20:347–356
- Kraines SB, Yanagi T, Isobe M, Komiyama H (1998) Wind-wave driven circulation on the coral reef at Bora Bay, Miyako Island. *Coral Reefs* 17:133–143
- Lugo-Fernández A, Roberts HH, Wiseman WJ, Carter BL (1998) Water level and currents of tidal and infragravity periods at Tague Reef, St. Croix (USVI). *Coral Reefs* 17:343–349
- Merino-Ibarra M, Otero-Dávalos L (1991) Atlas ambiental costero: Puerto Morelos, Quintana Roo. Centro de Investigaciones de Quintana Roo, Chetumal, Q.Roo., Mexico
- Pages J, Andréfouet S (2001) A reconnaissance approach for hydrology of atoll lagoons. *Coral Reefs* 20:409–414
- Pawlowicz R, Beardsley B, Lentz S (2002) Classical Tidal Harmonic Analysis Including Error Estimates in MATLAB using T\_TIDE. *Comput Geosci* 28:929–937
- Roberts HH, Wilson PA, Lugo-Fernández A (1992) Biologic and geologic responses to physical processes: examples from modern reef systems of the Caribbean-Atlantic region. *Cont Shelf Res* 12:809–834
- Ruíz-Rentería F, vanTussenbroek BI, Jordán-Dahlgren E (1998) CARICOMP—Caribbean coral reef, seagrass and mangrove sites: Puerto Morelos, Quintana Roo, México. *Coastal Regions and small island papers*. UNESCO, Paris
- Sheinbaum J, Candela J, Badan A, Ochoa J (2002) Flow structure and transport in the Yucatan Channel. *Geophys Res Lett* 29:1040
- Storlazzi CD, Ogston AS, Bothner MH, Field ME, Presto MK (2004) Wave- and tidally-driven flow and sedimentary flux across a fringing coral reef: Southern Molokai, Hawaii. *Cont Shelf Res* 24:1397–1419
- Symonds G, Black KP, Young IR (1995) Wave-driven flow over shallow reefs. *J Geophys Res* 100:2639–2648
- Tait RJ (1972) Wave set-up on coral reefs. *J Geophys Res* 77:2207–2211
- Tartinville B, Deleersnijder E, Rancher J (1997) The water residence time in the Mururoa atoll lagoon: sensitivity analysis of a three-dimensional model. *Coral Reefs* 16:193–203
- Wolanski E (1983) Tides on the northern Great Barrier Reef continental shelf. *J Geophys Res* 88:5953–5959
- Wolanski E (2001) *Oceanographic processes of coral reefs: physical and biological links in the Great Barrier Reef*. CRC Press, Boca Raton, FL
- Yamano H, Kayanne H, Yonekura N, Nakamura H, Kudo K (1998) Water circulation in a fringing reef located in a monsoon area: Kabira Reef, Ishigaki Island, Southwest Japan. *Coral Reefs* 17:89–99
- Young IR (1989) Wave transformation over coral reefs. *J Geophys Res* 94:9779–9789